

Ferrocenyl-Passivated Nanoclusters: Synthesis of $[\text{Cu}_{20}\text{Se}_6(\text{Se}_2\text{fc})_4(\text{PR}_2\text{R}')_{10}]$ and $[\text{Cu}_{40}\text{Se}_{12}(\text{Se}_2\text{fc})_8(\text{PPh}_3)_9]$

Andrew I. Wallbank,[†] Aneta Borecki,[†] Nicholas J. Taylor,[‡] and John F. Corrigan^{*,†}

Departments of Chemistry, The University of Western Ontario, London, Ontario N6A 5B7, Canada, and University of Waterloo, Waterloo, Ontario N2L 3G1, Canada

Received October 2, 2004

Summary: The reagent $\text{Fe}(\eta^5\text{-C}_5\text{H}_4\text{SeSiMe}_3)_2$ has been used for the formation of the new nanoclusters $[\text{Cu}_{20}\text{Se}_6(\text{Se}_2\text{fc})_4(\text{PR}_2\text{R}')_{10}]$ ($R = \text{Ph}$, $R' = \text{Et}$; $R = R' = n\text{Bu}$) and $[\text{Cu}_{40}\text{Se}_{12}(\text{Se}_2\text{fc})_8(\text{PPh}_3)_9]$, which consist of ferrocenyl-passivated surfaces on CuSe cores.

The assembly of complexes containing multiple ferrocenyl centers has been the focus of much attention, with the goal of preparing functional materials, including biosensors¹ and multielectron catalysts.² Recent work has illustrated the anion recognition ability of functionalized ferrocenyl-terminated nanoparticles¹ and how the tethering of ferrocenylalkylthiolate groups on Au nanoparticles can influence the intermolecular electron-transfer processes through the otherwise insulating ligand sheath.² It has also been demonstrated that the incorporation of ferrocene-based ligands onto metal–chalcogenide nanoparticles can have marked effects on the optical properties of the semiconductor³ and that the incorporation of multiple redox centers on such particles may lend itself to the control of their photo-physics, with potential utility in optical switching devices.⁴ To this end, we are interested in developing synthetic methodologies that will allow for the generation of well-defined semiconductor nanostructures whose surfaces contain multiple ferrocene sites. Herein we describe the first examples of structurally characterized metal–selenide nanoclusters whose surfaces are partly passivated by ferrocenyl ligands.

Silylated selenium reagents offer the advantage for the synthesis of metal–selenide nanoscale architectures that the highly soluble reagents enable homogeneous reaction conditions to be achieved, which is important for the formation and crystallization of larger complexes. Similarly, the silane byproduct generated does not interfere with the crystallization of the forming nanoclusters.⁵ A combination of chalcogenolate (RE^-) and chalcogenide (E^{2-}) reagents can allow for the formation

of a metal–chalcogenide core which can then be passivated via the introduction of surface chalcogenolate ligands.⁶ The synthesis of the ferrocenyl reagent $\text{Fe}(\eta^5\text{-C}_5\text{H}_4\text{SeSiMe}_3)_2$ ($\text{fc}(\text{SeSiMe}_3)_2$)⁷ thus offers a route for the formation of ferrocenyl-capped nanoclusters in which the redox-active iron center is proximal to the nanocluster core and for which structural characterization is possible. The development of approaches to access such functionalized particles is an attractive pursuit, as nanocluster materials whose structures can be determined crystallographically allow an investigation of the development of materials properties from the molecular size regime.⁸

The low-temperature reaction⁹ of $(\text{EtPh}_2\text{P})_3\text{-CuOAc}$, $\text{Se}(\text{SiMe}_3)_2$, and $\text{Fe}(\eta^5\text{-C}_5\text{H}_4\text{SeSiMe}_3)_2$ (10:3:2) leads to the high-yield formation of the cluster $[\text{Cu}_{20}\text{Se}_6(\text{Se}_2\text{fc})_4(\text{PPh}_2\text{Et})_{10}]$ (**1a**) as single crystals. The cluster resides on a crystallographic inversion center.¹⁰ The selenium framework in **1a** consists of two sets of three μ_5 -selenide ligands (Se5, Se6, Se7, and their symmetry equivalents) at the “top” and “bottom” of the clusters, which, in addition to the central ring of ferrocenyl selenolate groups, are bonded to the copper(I) centers. Of the organochalcogen ligands, Se1/Se1A act as μ_4 bridges, while the other six selenolate ligands each bond to three copper sites. The $\sim 1 \text{ nm}^3$ core of **1a** (Figure 1) can be

(6) (a) Corrigan, J. F.; Fenske, D. *J. Chem. Soc., Chem. Commun.* **1997**, 1837. (b) Eichhöfer, A.; Aharoni, A.; Banin, U. *Z. Anorg. Allg. Chem.* **2002**, 628, 2415. (c) Steigerwald, M. L.; Alivisatos, A. P.; Gibson, J. M.; Harris, T. D.; Kortan, R.; Muller, A. J.; Thayer, A. M.; Duncan, T. M.; Douglass, D. C.; Brus, L. E. *J. Am. Chem. Soc.* **1988**, 110, 3046.

(7) Wallbank, A. I.; Corrigan, J. F. *Chem. Commun.* **2001**, 377.

(8) (a) DeGroot, M. W.; Corrigan, J. F. In *The Chemistry of Nanomaterials: Synthesis, Properties and Applications*; Rao, C. N. R., Müller, A., Cheetham, A. K., Eds.; Wiley-VCH: Weinheim, Germany, 2004; Chapter 13. (b) Soloviev, V. N.; Eichhöfer, A.; Fenske, D.; Banin, U. *J. Am. Chem. Soc.* **2001**, 123, 2354.

(9) **Synthesis of 1a:** CuOAc (0.40 g, 3.26 mmol) was dissolved with PPh_2Et (1.35 mL, 6.53 mmol) in THF (10 mL). The solution was cooled to -70°C , and $\text{Se}(\text{SiMe}_3)_2$ (0.21 mL, 0.98 mmol) and a solution of $\text{fc}(\text{SeSiMe}_3)_2$ (0.318 g, 0.65 mmol in 2 mL of THF) were added. Slow warming to -25°C followed by slow progression from -25°C to room temperature over a period of days afforded a brown-red solution. Slow diffusion of pentane into the solution afforded crystals of **1a** in 67% yield. Anal. Calcd (found) for **1a**: C, 41.14 (41.55); H, 3.49 (3.51). **Synthesis of 1b:** CuOAc (0.40 g, 3.26 mmol) was dissolved with PBu_3 (6.53 mmol) in THF (10 mL). The solution was cooled to -70°C , and $\text{Se}(\text{SiMe}_3)_2$ (0.21 mL, 0.98 mmol) and a solution of $\text{fc}(\text{SeSiMe}_3)_2$ (0.318 g, 0.65 mmol in 2 mL of THF) were added. Slow warming to room temperature afforded a brown-red solution, and removal of the solvent in vacuo yielded a red-brown oil. Addition of pentane to dissolve the oil and subsequent slow evaporation gave X-ray-quality crystals of **1b** in 65% yield. Anal. Calcd (found) for **1b**: C, 37.42 (37.26); H, 5.93 (5.91). ¹H NMR (ferrocenyl region, C_7H_8 , δ): 5.28 (s, 1H), 5.11 (s, 1H), 5.09 (s, 1H), 4.61 (s, 1H), 4.27 (s, 1H), 4.23 (s, 1H), 4.17 (s, 1H), 4.09 (br s, 3H), 3.96 (br, 4H), 3.88 (br s, 2H). UV–vis (THF): increasing absorbance from λ_{onset} 610 nm.

* To whom correspondence should be addressed. E-mail: corrigan@uwo.ca.

[†] The University of Western Ontario.

[‡] University of Waterloo.

(1) Labande, A.; Ruiz, J.; Astruc, D. *J. Am. Chem. Soc.* **2002**, 124, 1782.

(2) (a) Ingram, K. S.; Hostetler, M. J.; Murray, R. W. *J. Am. Chem. Soc.* **1997**, 119, 9175. (b) Uosaki, K.; Kondo, T.; Okamura, M.; Song, W. *Faraday Discuss.* **2002**, 121, 373.

(3) Chandler, R. R.; Coffey, J. L.; Atherton, S. J.; Snowden, P. T. *J. Phys. Chem. B* **1992**, 96, 2713.

(4) Cyr, P. W.; Tzolov, M.; Hines, M. A.; Manners, I.; Sargent, E. H.; Scholes, G. D. *J. Mater. Chem.* **2003**, 13, 2213.

(5) Dehnen, S.; Eichhöfer, A.; Fenske, D. *Eur. J. Inorg. Chem.* **2002**, 2, 279.

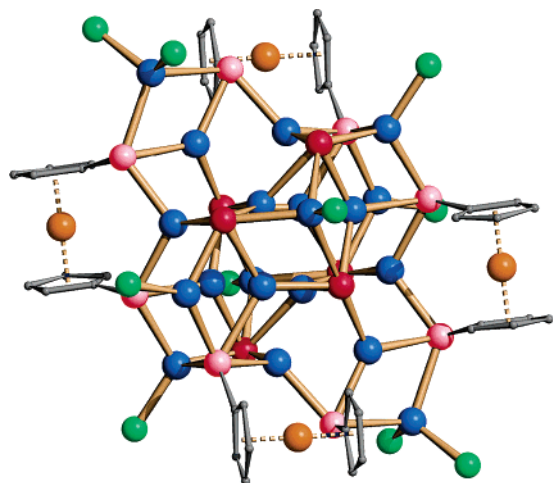


Figure 1. Molecular structure of $[\text{Cu}_{20}\text{Se}_6(\text{Se}_2\text{fc})_4(\text{PPh}_2\text{Et})_{10}]$ (**1a**). The ball-and-stick representation (copper, blue; iron, orange; selenide, dark red; selenolate, light red; phosphorus, green; carbon, gray) omits the hydrogen atoms and the substituents of the phosphine ligands for clarity. Selected bond lengths (Å): $\mu_3\text{-SeC}_5\text{H}_4\text{-Cu}$, 2.398(1)–2.608(1); $\mu_4\text{-SeC}_5\text{H}_4\text{-Cu}$, 2.428(1)–2.788(1); $\mu_5\text{-Se-Cu}$, 2.387(1)–2.704(1) Å.

contrasted with the open framework observed in the smaller copper–selenolate cluster $[\text{Cu}_8(\text{Se}_2\text{fc})_4(\text{PPh}_2\text{Et})_4]$, which is formed in the absence of any Se^{2-} .⁷ The ferrocenyl units, which are ‘exposed’ at the surface of the cluster, are sandwiched between 10 phosphine ligands (Figure 1). The copper centers display a mixture of trigonal and tetrahedral coordination geometries. The same CuSe framework in **1a** is repeated in the isostructural¹⁰ cluster $[\text{Cu}_{20}\text{Se}_6(\text{Se}_2\text{fc})_4(\text{PnBu}_3)_{10}]$ (**1b**). In **1b** the tributylphosphine ligands impart greater solubility to the $\text{Cu}_{20}\text{Se}_6(\text{Se}_2\text{fc})_4$ framework. The cluster framework in **1b** displays long-term stability in solution, as monitored by NMR spectroscopy and dynamic light scattering experiments. We attribute this to the bidentate nature of the ferrocenyl diselenolate ligands on the cluster surface.

The incorporation of an even larger number of central selenide ligands allows for correspondingly larger metal–selenium complexes to be formed. Thus, a reaction similar to the synthesis of **1a** and **1b** with $(\text{Ph}_3\text{P})_3\text{CuOAc}$, $\text{Se}(\text{SiMe}_3)_2$, and $\text{Fe}(\eta^5\text{-C}_5\text{H}_4\text{SeSiMe}_3)_2$ (10:3:2) leads to the selective formation of the nanocluster $[\text{Cu}_{40}$ -

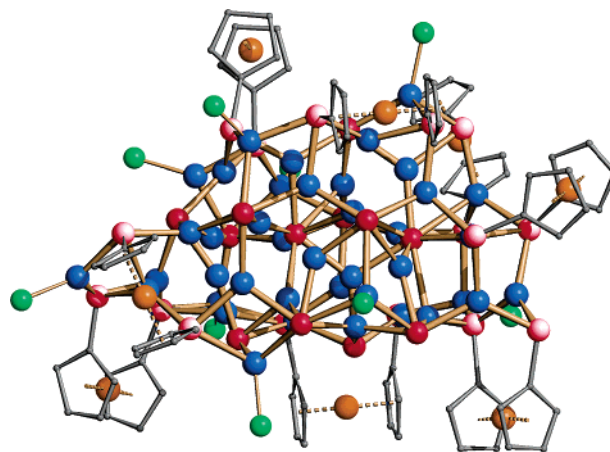


Figure 2. Molecular structure of $[\text{Cu}_{40}\text{Se}_{12}(\text{Se}_2\text{fc})_8(\text{PPh}_3)_9]$ (**2**). The ball-and-stick representation (copper, blue; iron, orange; selenide, dark red; selenolate, light red; phosphorus, green; carbon, gray) omits the hydrogen atoms and the substituents of the phosphine ligands for clarity. Selected bond lengths (Å): $\mu_2\text{-SeC}_5\text{H}_4\text{-Cu}$, 2.315(2)–2.371(2); $\mu_3\text{-SeC}_5\text{H}_4\text{-Cu}$, 2.328(2)–2.702(2); $\mu_4\text{-SeC}_5\text{H}_4\text{-Cu}$, 2.449(2)–2.667(2); $\mu_4\text{-Se-Cu}$, 2.394(2)–2.422(2); $\mu_5\text{-Se-Cu}$, 2.305(2)–2.585(2); $\mu_6\text{-Se-Cu}$, 2.378(2)–2.683(2); $\mu_7\text{-Se-Cu}$, 2.297(2)–2.748(2); $\mu_8\text{-Se-Cu}$, 2.414(2)–2.898(2) Å.

$\text{Se}_{12}(\text{Se}_2\text{fc})_8(\text{PPh}_3)_9]$ (**2**),¹¹ the structure of which consists of a $\sim 1.3 \times 1.0 \times 1.0 \text{ nm}^3$ CuSe core (Figure 2).¹⁰ In **2**, 12 Se^{2-} centers are distributed through the cluster and 8 ferrocenyl groups occupy positions on the surface of the core. The bidentate nature of the ferrocenyl selenolate ligands results in little overall structural resemblance to reported copper–selenide–selenolate nanoclusters, and **2** is less symmetrical than structures observed for similarly sized Cu/Se/SeR complexes.⁵ The surface of the cluster is terminated by the 16 $\mu_{2/3/4}\text{-SeC}_5\text{H}_4$ and 9 PPh_3 groups. Consistent with the more highly condensed copper–selenide core, the Se^{2-} ligands in **2** are $\mu_4\text{-}\mu_8$ -bonded to the metal centers, the majority of Cu(I) atoms being located within the three selenium layers. The selenium substructure in **2** is best described as comprised of ABC type packing.

The ease of synthesis of clusters **1a**, **1b**, and **2** suggests the general utility of $\text{Fe}(\eta^5\text{-C}_5\text{H}_4\text{SeSiMe}_3)_2$ and $\text{CpFe}(\eta^5\text{-C}_5\text{H}_4\text{SeSiMe}_3)$ ¹² for the assembly of high-nuclearity metal–chalcogen clusters containing multiple ferrocenyl centers. We are currently developing this methodology for the general synthesis of metal–chalcogenide–ferrocenylchalcogenolate nanocluster and nanoparticle complexes and investigating the effect of the organometallic surfaces on their physical and electrochemical properties.

Acknowledgment. We gratefully acknowledge the Natural Sciences and Engineering Research Council

(10) Crystal data for $\text{C}_{180}\text{H}_{182}\text{Cu}_{20}\text{Fe}_4\text{P}_{10}\text{Se}_{14}\cdot 8\text{OC}_4\text{H}_8$ (**1a**): red needle, $M_r = 5831.43$, triclinic, space group $P1$, $a = 17.6298(4)$ Å, $b = 18.2844(3)$ Å, $c = 19.0130(5)$ Å, $\alpha = 79.948(1)^\circ$, $\beta = 89.293(1)^\circ$, $\gamma = 63.643(1)^\circ$, $V = 5392.7(2)$ Å³, at 200 K, $Z = 1$, $\rho_{\text{calcd}} = 1.796 \text{ g cm}^{-3}$, $\mu = 4.674 \text{ mm}^{-1}$, $2\theta_{\text{max}} = 50.0^\circ$, 28 154 reflections collected (18 927 independent, $R_{\text{int}} = 0.062$), final $R1 = 0.0597$ ($wR2 = 0.1068$) and $\text{GOF} = 0.922$. Crystal data for $\text{C}_{160}\text{H}_{302}\text{Cu}_{20}\text{Fe}_4\text{P}_{10}\text{Se}_{14}$ (**1b**): brown-red polyhedron, $M_r = 8729.23$, monoclinic, space group $P2_1/n$, $a = 19.550(1)$ Å, $b = 18.969(1)$ Å, $c = 26.596(2)$ Å, $V = 9730(1)$ Å³, at 150 K, $Z = 2$, $\rho_{\text{calcd}} = 1.753 \text{ g cm}^{-3}$, $\mu = 5.164 \text{ mm}^{-1}$, $2\theta_{\text{max}} = 60.1^\circ$, 120 515 reflections (28 487 independent, $R_{\text{int}} = 0.044$), final $R1 = 0.0311$ ($wR2 = 0.0518$) and $\text{GOF} = 1.083$. Crystal data for $\text{C}_{242}\text{H}_{199}\text{Cu}_{40}\text{Fe}_8\text{P}_9\text{Se}_{28}\cdot (\text{OC}_4\text{H}_8)_2$ (**2**): brown block, $M_r = 8729.23$, monoclinic, space group $P2_1/n$, $a = 21.1482(3)$ Å, $b = 29.3806(5)$ Å, $c = 49.789(8)$ Å, $V = 30797(5)$ Å³, at 200 K, $Z = 4$, $\rho_{\text{calcd}} = 1.883 \text{ g cm}^{-3}$, $\mu = 6.455 \text{ mm}^{-1}$, $2\theta_{\text{max}} = 48.2^\circ$, 131 477 reflections (48 481 independent, $R_{\text{int}} = 0.076$), final $R1 = 0.0563$ ($wR2 = 0.1866$) and $\text{GOF} = 1.065$. CCDC files 237560 and 237561 contain the supplementary crystallographic data for **1a** and **2**. These data can be obtained online free of charge (or from the Cambridge Crystallographic Data Centre, 12, Union Road, Cambridge CB2 1EZ, U.K.; fax, (+44) 1223-336-033; e-mail, deposit@ccdc.cam.ac.uk).

(11) *Synthesis of 2*: CuOAc (0.35 g, 2.85 mmol) was dissolved with PPh_3 (1.50 g, 5.71 mmol) in THF (30 mL). The solution was cooled to -70°C , and $\text{Se}(\text{SiMe}_3)_2$ (0.19 mL, 0.86 mmol) and a solution of $\text{Fe}(\text{SiMe}_3)_2$ (0.279 g, 0.57 mmol in 2 mL of THF) were added. Slow warming of the solution to -25°C followed by slow progression from -25°C to room temperature over a period of days afforded a brown-red solution. Slow diffusion of pentane (20 mL) into the solution afforded crystals of **2** in 62% yield. Anal. Calcd (found) for **2**·2THF: C, 34.4 (34.31); H, 2.48 (2.80).

(12) Lebold, T. P.; Stringle, D. L. B.; Workentin, M. S.; Corrigan, J. F. *Chem. Commun.* **2003**, 1398.

(NSERC) of Canada and the Government of Ontario (PREA program) for financial support of this research. The Canada Foundation for Innovation, the Ontario Research Development and Challenge Fund, the NSERC, and The University of Western Ontario are also acknowledged for equipment funding. A.I.W. thanks the Government of Ontario for a postgraduate scholarship.

Supporting Information Available: Tables giving crystallographic data, including full listings of bond lengths and angles, for **1a**, **1b**, and **2**; these data are also available as CIF files. This material is available free of charge via the Internet at <http://pubs.acs.org>.

OM049238C